J|A|C|S
ARTICLES
Published on Web 04/04/2006

Nanostructured Oligo(*p*-phenylene Vinylene)/Silicate Hybrid Films: One-Step Fabrication and Energy Transfer Studies

Keisuke Tajima,† Liang-shi Li, and Samuel I. Stupp*

Contribution from the Department of Chemistry, Department of Materials Science and Engineering, Feinberg School of Medicine, Northwestern University, Evanston, Illinois 60208

Received December 20, 2005; E-mail: s-stupp@northwestern.edu

Abstract: Novel hybrid materials containing silicate and charged oligo(*p*-phenylene vinylene) (OPV) amphiphiles were fabricated in one step by spin casting using evaporation-induced self assembly. The conjugated segments were substituted with trimethylammonium bromide groups at both termini, and tetraethyl orthosilicate served as the silicate precursor. X-ray diffraction scans of the hybrid films revealed Bragg diffraction peaks with *d*-spacings of 2.76 and 1.37 nm, indicating the presence of order in the hybrid structure. Optical properties of the hybrid films were characterized by UV−vis absorption and fluorescence spectra, and molecular orientation was characterized by IR spectroscopy. A rhodamine B derivative containing a triethoxysilane group was covalently incorporated into the silicate network of the films during the sol−gel reaction. Relative to disordered polymer films with identical organic composition, the ordered hybrid films revealed significantly enhanced emission from rhodamine B and also fluorescence quenching from OPV segments. These results indicate that the ordered and nanostructured environment leads to highly efficient energy transfer among organic components in these hybrid films.

Introduction

Light-harvesting complexes in green plants and some bacteria are good examples for showing the importance of spatial molecular arrangements in controlling the direction and efficiency of electron or energy transfer.[1] Inspired by these systems, many studies have been carried out to introduce structural order in semiconducting organic materials to control charge transport and energy transfer processes, especially for the goal of developing high performance devices such as field effect transistors (FETs)[2] or organic solar cells.[3] Fabrication techniques such as Langmuir−Blodgett (LB) methodology[4] or layer-by-layer deposition[5] offer the possibility of controlling nanoscale structure and molecular orientation in organic materials. For example, Swager et al. reported previously on multilayer LB films of conjugated polymers with different band gaps to achieve directional energy transfer in thin films.[4b] While these fabrication techniques provide ways to achieve structural order at the nanometer scale, they involve multistep processes that are not easily scalable and may be difficult to implement in the context of device fabrication. It is therefore highly desirable to investigate what self assembly may offer to create materials with interesting optical and electronic properties. Meijer and coworkers reported that chiral oligo(*p*-phenylene vinylene) (OPV) molecules self assembled to form helical stacking structures in solution.[6] Very recently, they reported that structural order in the self-assembled helix significantly affects the efficiency of energy transfer between OPVs.[7]

We report here on a strategy for the one-step fabrication of a nanostructured hybrid material containing OPV segments and silicate. Our strategy takes advantage of "evaporation-induced self assembly" developed recently by Brinker et al. to synthesize mesoporous silicate films.[8,9] In this method, the hydrophilic segments of amphiphilic molecules interact with precursors for inorganic materials and self assemble into ordered phases such

† Current address: Department of Applied Chemistry, School of Engineering, The University of Tokyo, 7−3−1 Hongo, Bunkyo-ku, Tokyo 113-8656, Japan.

(1) (a) Oijen, A. M. V.; Ketelaars, M.; Kohler, J.; Aartsma, T. J.; Schmidt, J. *Science* **1999**, *285*, 400−402. (b) Hu, X.; Damjanovic, A.; Ritz, T.; Schulten, K. *Proc. Natl. Acad. Sci. U.S.A.* **1998**, *95*, 5935−5941.
(2) Sirringhaus, H.; Brown, P. J.; Friend, R. H.; Nielsen, M. M.; Bechgaard, K.; Langeveld-Voss, B. M. W.; Spiering, A. J. H.; Janssen, R. A. J.; Meijer, E. W.; Herwig, P.; Leeuw, D. M. d. *Nature* **1999**, *401*, 685.
(3) (a) Schmidt-Mende, L.; Fechtenkotter, A.; Mullen, K.; Moons, E.; Friend, R. H.; MacKenzie, J. D. *Science* **2001**, *293*, 1119−1122. (b) Granstrom, M.; Petritsch, K.; Arias, A. C.; Lux, A.; Andersson, M. R.; Friend, R. H. *Nature* **1998**, *395*, 257−260.
(4) (a) Kim, J.; McQuade, D. T.; Rose, A.; Zhu, Z.; Swager, T. M. *J. Am. Chem. Soc.* **2001**, *123*, 11488−11489. (b) Kim, J.; Levitsky Igor, A.; McQuade, D. T.; Swager Timothy, M. *J. Am. Chem. Soc.* **2002**, *124*, 7710−8. (c) Hill, J.; Heriot, S. Y.; Worsfold, O.; Richardson, T. H.; Fox, A. M. *Phys. Rev. B: Condens. Matter Mater. Phys.* **2004**, *69*, 041303−1. (d) Matsui, J.; Abe, K.-i.; Mitsuishi, M.; Miyashita, T. *Mol. Cryst. Liq. Cryst.* **2004**, *424*, 187−194. (e) Sakomura, M.; Ueda, K.; Fujihara, M. *Chem. Commun.* **2004**, 2392−2393.
(5) (a) Sun, J.; Sun, J.; Ma, Y.; Zhang, X.; Shen, J. *Mater. Sci. Eng., C* **1999**, C10, 83−86. (b) Lin, C.; Kagan, C. R. *J. Am. Chem. Soc.* **2003**, *125*, 336−337. (c) Richter, B.; Kirstein, S. *J. Chem. Phys.* **1999**, *111*, 5191−5200. (d) Fushimi, T.; Oda, A.; Ohkita, H.; Ito, S. *J. Phys. Chem. B* **2004**, *108*, 18897−18902. (e) Franzl, T.; Koktysh, D. S.; Klar, T. A.; Rogach, A. L.; Feldmann, J. *Appl. Phys. Lett.* **2004**, *84*, 2904−2906. (f) van der Boom, M. E.; Evmenenko, G.; Yu, C.; Dutta, P., Marks, T. J. *Langumuir* **2003**, *19*, 10531−10537.
(6) (a) Schenning, A.; Jonkheijm, P.; Peeters, E.; Meijer, E. W. *J. Am. Chem. Soc.* **2001**, *123*, 409−416. For reviews on self-assembled π-conjugated systems, see: (b) Hoeben, F. J. M.; Jonkheijm, P.; Meijer, E. W.; Schenning, A. *Chem. Rev.* **2005**, *105*, 1491−1546. (c) Schenning, A.; Meijer, E. W. *Chem. Commun.* **2005**, 3245−3258.
(7) (a) Hoeben, F. J. M.; Herz, L. M.; Daniel, C.; Jonkheijm, P.; Schenning, A.; Silva, C.; Meskers, S. C. J.; Beljonne, D.; Phillips, R. T.; Friend, R. H.; Meijer, E. W. *Angew. Chem., Int. Ed.* **2004**, *43*, 1976−1979. (b) Hoeben, F. J. M.; Schenning, A.; Meijer, E. W. *Chemphyschem* **2005**, *6*, 2337−2342.

10.1021/ja058610s CCC: $33.50

as cubic, hexagonal, or lamellar structures during solvent evaporation. We designed the amphiphilic molecules with OPV segments that have good chemical stability as well as high electroluminescence and hole conductivity.[10] OPV is therefore an interesting target for both organic light emitting diodes (OLEDs) and organic solar cells. The synthesis of a PPV/silicate composite material has been previously reported using soluble PPV precursor polymers and silicon alkoxides for the sol−gel process;[11] however, structural order is not expected in these polymer-silicate mixtures. Nanostructured PPV/clay films have also been fabricated using a layer-by-layer deposition technique, and in this case, enhanced stability of the films toward UV irradiation was reported.[12] Our work here investigates the use of self-assembling molecules to create highly ordered and nanostructured films based on OPV and silicate in one step. OPV segments are especially useful for the design of self-assembling molecules given their tendency to aggregate through $\pi-\pi$ stacking interactions.[13] We use here an amphiphilic compound containing OPV segments as opposed to polymeric components to generate highly ordered structures. An amphiphile was used given the well-known tendency for surfactants to form ordered phases. Furthermore, a "strongly amphiphilic" charged compound was selected to raise the probability that ordered phases would not be disrupted by the introduction of precursors for inorganic materials. This would then offer the possibility of one-step formation of a highly ordered hybrid material. Hybrid films formed through self assembly are extremely important model structures to understand how nanoscale order parameters influence electronic properties. In this paper, we address this question by modifying the system with a rhodamine B derivative and probing energy transfer in the hybrid films.

Results and Discussion

Synthesis. We were able to synthesize OPV amphiphiles **1** (Figure 1) using the Horner−Emmons reaction for the formation of *trans*-vinyl bonds and subsequent methylation of the dimethylamines to the tetramethylammonium salts. **1a** ($n = 2$) was found to be readily soluble in MeOH, whereas **1b**−**d**, with

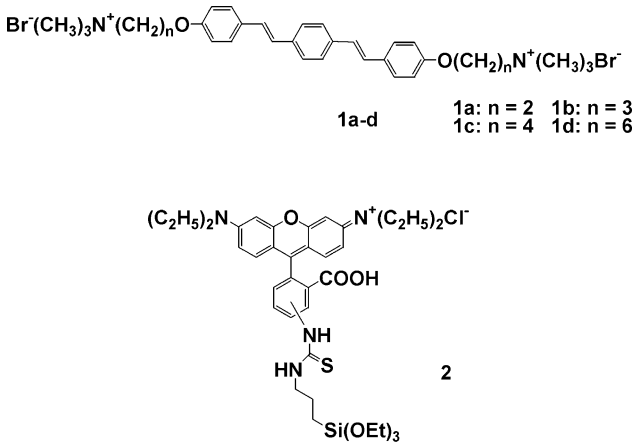

Figure 1. Chemical structures of oligo(*p*-phenylene vinylene) amphiphiles (**1**) and of the rhodamine B derivative used in the formation of the silicate domain (**2**).

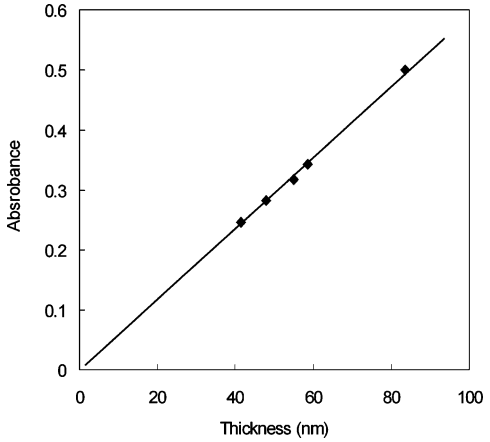

Figure 2. Plot of film thickness as a function of absorbance at 350 nm by oligo(*p*-phenylene vinylene) segments in **1a**/silicate films.

longer alkyl linkers, had lower solubilities relative to **1a**. Because MeOH is a good solvent for the silicate precursor tetraethyl orthosilicate (TEOS) and its hydrolyzing agent HCl, we were able to create hybrid films of **1a** and silicate by simply spin casting MeOH solutions on a variety of substrates such as silicon, quartz, and glass. The films obtained by spin casting solutions were macroscopically homogeneous and transparent with thicknesses on the order of 40−80 nm.

Characterization of Hybrid Films. The thickness of hybrid films was found to be controlled by rotation speed used during spin casting. We also found a linear relationship between optical density measured by UV−vis absorption and film thickness determined by ellipsometry (Figure 2), suggesting a uniform distribution of the amphiphile in the hybrid films. Small-angle X-ray diffraction (XRD) scans of **1a**/silicate films spin cast at 2000 rpm revealed peaks at 2.76 and 1.37 nm (Figure 3), indicating the presence of a periodic structure in the hybrid film. The *d*-spacing of 2.76 nm is slightly larger than the length of a fully extended molecule of **1a** (calculated distance between two nitrogens in **1a** is 2.5 nm). When we used OPV amphiphiles with longer alkyl spacers of $n = 3$ (**1b**) and $n = 4$ (**1c**), the *d*-spacing of **1**/silicate films increased to 3.0 and 3.3 nm, respectively. However, the OPV amphiphile with $n = 6$ (**1d**) yielded an inhomogeneous, opaque film because of its low solubility in MeOH. The results obtained with **1b** and **1c** indicate that the periodicity observed in the film is directly controlled

(8) For recent reviews, see: (a) Fan, H.; Brinker, J. *Stud. Surf. Sci. Catal.* **2004**, *148*, 213−240. (b) Brinker, C. J.; Lu, Y.; Sellinger, A.; Fan, H. *Adv. Mater.* **1999**, *11*, 579−585. For synthesis of mesoporous silicate films, see: (c) Beck, J. S.; Vartuli, J. C.; Roth, W. J.; Leonowicz, M. E.; Kresge, C. T.; Schmitt, K. D.; Chu, C. T. W.; Olson, D. H.; Sheppard, E. W.; McCullen, S. B.; Higgins, J. B.; Schlenker, J. L. *J. Am. Chem. Soc.* **1992**, *114*, 10834−10843. (d) Ogawa, M. *Chem. Commun.* **1996**, 1149−1150. (e) Yang, H.; Coombs, N.; Sokolov, I.; Ozin, G. A. *Nature* **1996**, *381*, 589−592. (f) Lu, Y. F.; Ganguli, R.; Drewien, C. A.; Anderson, M. T.; Brinker, C. J.; Gong, W. L.; Guo, Y. X.; Soyez, H.; Dunn, B.; Huang, M. H.; Zink, J. I. *Nature* **1997**, *389*, 364−368.

(9) (a) Aida, T.; Tajima, K. *Angew. Chem., Int. Ed.* **2001**, *40*, 3803−3806. (b) Ikegame, M.; Tajima, K.; Aida, T. *Angew. Chem., Int. Ed.* **2003**, *42*, 2154−2157. (c) Li, G.; Bhosale, S.; Wang, T.; Zhang, Y.; Zhu, H.; Fuhrhop, J.-H. *Angew. Chem., Int. Ed.* **2003**, *42*, 3818−3821. (d) Lu, Y. F.; Yang, Y.; Sellinger, A.; Lu, M. C.; Huang, J. M.; Fan, H. Y.; Haddad, R.; Lopez, G.; Burns, A. R.; Sasaki, D. Y.; Shelnutt, J.; Brinker, C. J. *Nature* **2001**, *410*, 913−917. (e) Yang, Y.; Lu, Y.; Lu, M.; Huang, J.; Haddad, R.; Xomeritakis, G.; Liu, N.; Malanoski, A. P.; Sturmayr, D.; Fan, H.; Sasaki, D. Y.; Assink, R. A.; Shelnutt, J. A.; van Swol, F.; Lopez, G. P.; Burns, A. R.; Brinker, C. J. *J. Am. Chem. Soc.* **2003**, *125*, 1269−1277. (f) Honma, I.; Zhou, H. S. *Adv. Mater.* **1998**, *10*, 1532−1536.

(10) (a) Burroughes, J. H.; Bradley, D. D. C.; Brown, A. R.; Marks, R. N.; Mackay, K.; Friend, R. H.; Burns, P. L.; Holmes, A. B. *Nature* **1990**, *347*, 539−41. (b) Wong, M. S.; Li, Z. H.; Shek, M. F.; Chow, K. H.; Tao, Y.; D'Iorio, M. *J. Mater. Chem.* **2000**, *10*, 1805−1810. (c) Hulvat, J. F.; Sofos, M.; Tajima, K.; Stupp, S. I. *J. Am. Chem. Soc.* **2004**, *127*, 366−372.

(11) Chang, W.-P.; Whang, W.-T. *Polymer* **1996**, *37*, 4229.

(12) Lee, H.-C.; Lee, T.-W.; Park, O. O. *Opt. Mater.* **2002**, *21*, 187−190.

(13) Tew, G. N.; Pralle, M. U.; Stupp, S. I. *J. Am. Chem. Soc.* **1999**, *121*, 9852−9866.

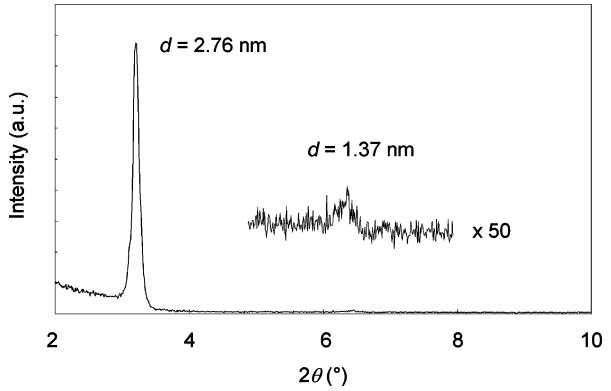

Figure 3. X-ray diffraction pattern of the hybrid oligo(*p*-phenylene vinylene) amphiphile (**1a**)/silicate film.

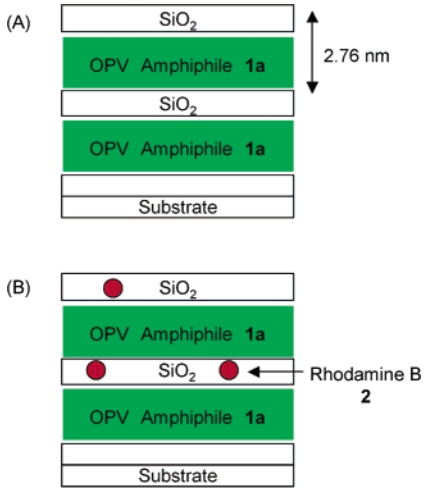

Figure 4. (A) Schematic representation of possible structure in oligo(*p*-phenylene vinylene) amphiphile (**1a**)/silicate films and (B) similar films when doped with the rhodamine B derivative (**2**). Organic OPV domains may also contain some silica.

by the dimensions of the amphiphilic molecule. When the molar ratio of **1a** to TEOS in the precursor solution was lowered from 0.15 to 0.08, the intensity of the first peak was decreased with little change in *d*-spacing (2.70 nm). At a lower ratio of 0.05, X-ray diffraction peaks are no longer observed. We conclude from these results that OPV domains in the hybrid films are separated by layers of silicate which do not grow significantly as the concentration of TEOS is increased. This implies that the silicate layers in the hybrid films are thin and have a self-limiting thickness. Therefore, increasing TEOS concentration simply generates silicate that is not part of the periodic hybrid structure, explaining why the diffraction peaks disappear at high TEOS concentration. The *d*-spacings of 2.76 and 1.37 nm can be assigned to (001) and (002) diffractions of a layered structure, respectively. However, these *d*-spacings could correspond also to (100) and (200) diffractions of a hexagonal structure aligned parallel to the substrate. This has been observed in mesoporous silica films in which orientation of the hexagonal structure parallel to the substrate precludes observation of the (110) diffraction.[14] Detailed structural analysis of these films is currently underway using synchrotron X-ray experiments. The structure of the hybridized film is proposed in Figure 4A schematically.

To determine molecular orientation in the hybrid films, we obtained infrared (IR) transmittance spectra of the **1a**/silicate films deposited on undoped silicon substrates (Figure 5A). We used the IR spectrum of an isotropic sample (Figure 5B), which is prepared by scraping off the hybrid film from the substrate and dispersing it into a KBr pellet, as a standard for a random orientation. By comparing these two spectra, we can estimate the orientation of the OPV segments in the hybrid films. Peaks at 1602 cm^{-1} and 962 cm^{-1} are assigned to vibrational modes of the OPV segments corresponding to phenyl ring quadrant stretching (parallel to the axis of 1,4-substitution) and *trans*-vinyl C−H out-of-plane wagging (perpendicular to the phenyl plane), respectively.[15] We assume that the films are azimuthally isotropic and use the "partial symmetrical planar orientation" model.[16] The orientation of OPV segments in the film is calculated with the formula

$$\frac{A_{\text{sample},962}/A_{\text{sample},1602}}{A_{\text{random},962}/A_{\text{random},1602}} = \frac{2-F}{2F}$$

where A_{sample} and A_{random} are peak areas of absorptions in the hybrid film and the isotropic sample, respectively, and

$$F = \int_0^{2\pi} \sin^2\gamma \cdot f(\gamma)\mathrm{d}\gamma = \sin^2\theta$$

where θ is the average molecular angle of the OPV segments with respect to the film normal. From the IR spectra shown in Figure 5, we can obtain a peak ratio of 1.5; thus, $F = 0.5$ and $\theta = 45°$. This result leads to an order parameter of 0.25. Therefore, we can conclude that the OPV segments are not oriented with high-order parameter normal to the substrate, but at the same time, the segments do not have isotropic orientation in the hybrid films. The actual orientation of the molecules in these obviously periodic hybrid films will require further experiments in the future.

UV−vis absorption spectra of the **1a**/silicate films showed a broad peak with a maximum at 350 nm, showing a blue-shift relative to that of the peak obtained in a MeOH solution of **1a.** (362 nm) (Figure 6A). The corresponding fluorescence spectra are shown in Figure 6B. The maximum in the excitation spectra of **1a**/silicate films (356 nm) reveals a slight blue-shift relative to **1a** in MeOH (362 nm), while a red-shift from 400 to 450 nm is observed in emission spectra. Based on these spectroscopic measurements, we conclude that OPV segments of **1a** in the films stack into H aggregates held together by $\pi-\pi$ interactions within the organic domains (Figure 4A).

Energy Transfer in Hybrid Films. The periodic nanostructure in hybrid films offers the opportunity to investigate how its order parameters influence energy transfer. For this purpose, rhodamine B derivative **2** (Figure 1) was synthesized and introduced into the **1a**/silicate films as an energy acceptor.[17] The ethoxysilane groups of **2** participate in the formation of the silicate network during the film deposition, resulting in the formation of a periodic structure with organic domains of donor **1a** and silicate domains doped with acceptor **2** (schematically shown in Figure 4B).

(14) Hillhouse, H. W.; Egmond, J. W. v.; Tsapatsis, M.; Hanson, J. C.; Larese, J. Z. *Microporous Mesoporous Mater.* **2001**, *44*−*45*, 639−643.
(15) (a) Colthup, N. B.; Daly, L. H.; Wiberley, S. E. *Introduction to Infrared and Raman Spectroscopy*; Academic Press: New York, 1975. (b) Bradley, D. D. C.; Friend, R. H. *Polymer* **1986**, *27*, 1709−1713.
(16) R. Zbinden, *Infrared Spectroscopy of High Polymers*; Academic Press: New York and London, 1964; p 216.
(17) Verhaegh, N. A. M.; van Blaaderen, A. *Langmuir* **1994**, *10*, 1427−1438.

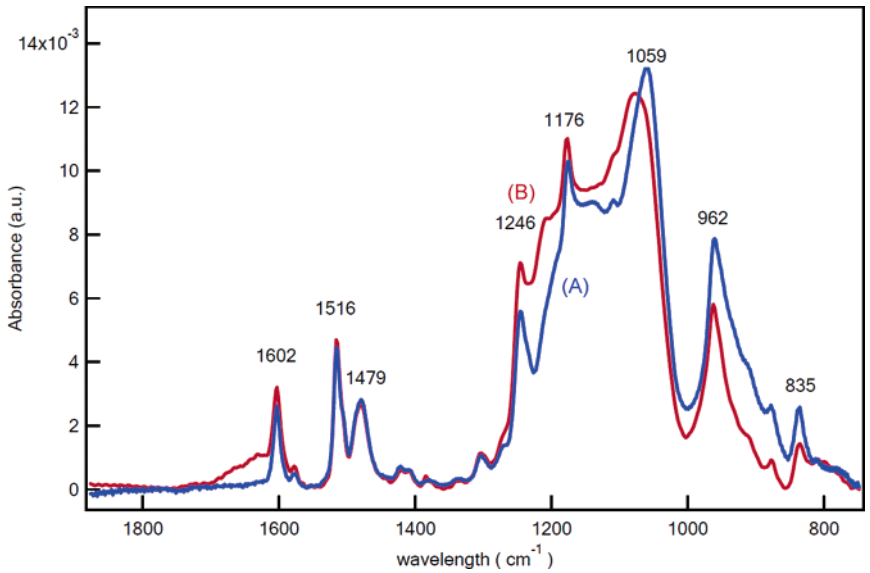

Figure 5. Infrared absorption spectra of (A) an oligo(*p*-phenylene vinylene) amphiphile (**1a**)/silicate film on a silicon substrate (blue line) and (B) the film scraped off from the substrate and dispersed in a KBr pellet (red line). The orientation of OPV segments in the film was estimated by comparing the ratio of the areas under the peaks at 1602 and 962 cm^{-1} (see main text).

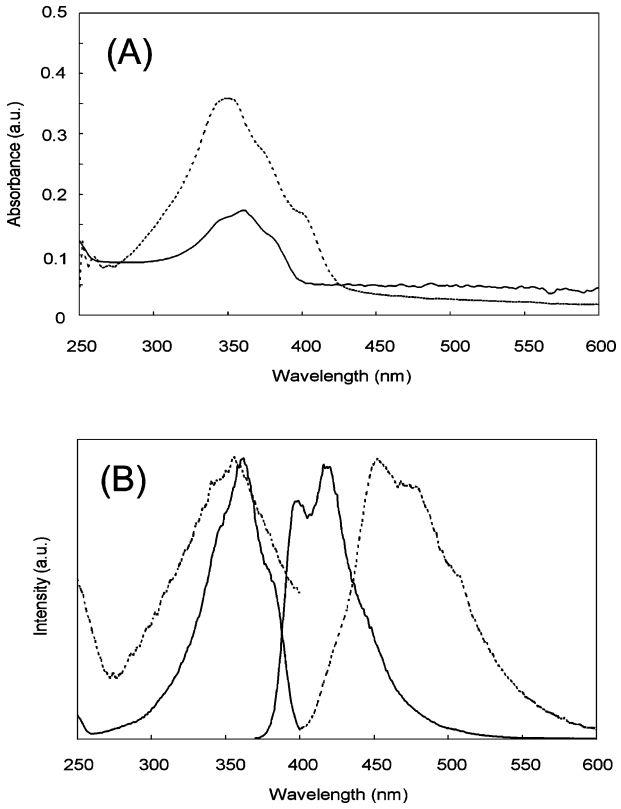

Figure 6. (A) UV−vis absorption spectra of oligo(*p*-phenylene vinylene) amphiphile (**1a**) in MeOH (solid line) and **1a**/silicate film (dashed line). (B) Excitation (left) and emission (right) fluorescence spectra of **1a** in MeOH (solid line, $\lambda_{em} = 418$ nm and $\lambda_{ex} = 350$ nm) and a **1a**/silicate film (dashed line, $\lambda_{em} = 452$ nm and $\lambda_{ex} = 350$ nm).

Precursor solutions for the hybrid films are prepared by adding the proper amounts of **2** while the concentrations of **1a** and silicate precursors in the solution are kept constant. The amount of **2** in precursor solutions was changed from 0.5 to 10 mol % with respect to the amount of **1a**.

XRD scans of the spin-cast films doped with up to 10 mol % of **2** showed a diffraction peak at 2.7 nm, indicating the presence of the periodic structure observed in undoped hybrid films. UV−vis absorption spectra of the films showed a peak around 560 nm corresponding to absorption by **2** in addition to the absorption by OPV segments (Figure 7A). The peak maxima red-shifted from 556 nm (0.5 mol %) to 572 nm (10 mol %) as the amount of **2** in the films was increased. This red-shift is assigned to the formation of dimeric species in the films, commonly observed at this concentration of the dye in silicate films.[18] The absorbance of **2** in the films was linear with the amount of **2** in the precursor solution as shown in Figure 7C, indicating that the rhodamine B derivative is incorporated homogeneously into the films up to a concentration of 10 mol %. Considering the XRD data and the absorption spectra, we conclude rhodamine B derivative **2** was successfully incorporated into the silicate network without disrupting the ordered structure.

Fluorescence spectra of the hybrid films doped with **2** are shown in Figure 8A. When the amount of **2** in the films was increased, fluorescence at 480 nm from OPV segments was quenched. The fluorescence intensity at 480 nm was plotted as a function of absorbance from **2** in Figure 8C.[19] This result clearly demonstrates that the introduction of **2** in the films caused efficient quenching of OPV fluorescence. At the same time, fluorescence from the rhodamine B derivative can be observed as films are doped with **2**. The fluorescence from **2** showed both a decrease in intensity and a red-shift of the peak maximum from 582 nm (0.5 mol %) to 605 nm (10 mol %) as the amount of **2** was increased. These observations can be explained by concentration quenching, which is an increase of the nonfluorescent dimeric species of **2** in the films.[18] Because **2** is not fluorescent with excitation at 350 nm, emission from **2** clearly indicates energy transfer occurs from **1a** to **2** in the hybrid films. This is further supported by the excitation spectrum of the hybrid film doped with **2** (Figure 9, red line). Emission

(18) (a) Valdes-Aguilera, O.; Neckers, D. C. *Acc. Chem. Res.* **1989**, *22*, 171−177. (b) Nishikiori, H.; Fujii, T. *J. Phys. Chem. B* **1997**, *101*, 3680−3687. (c) Fujii, T.; Nishikiori, H.; Tamura, T. *Chem. Phys. Lett.* **1995**, 233.

(19) The fluorescence intensities were corrected with the absorbance at 350 nm in the UV spectra, i.e., the amount of **1a** in the films.

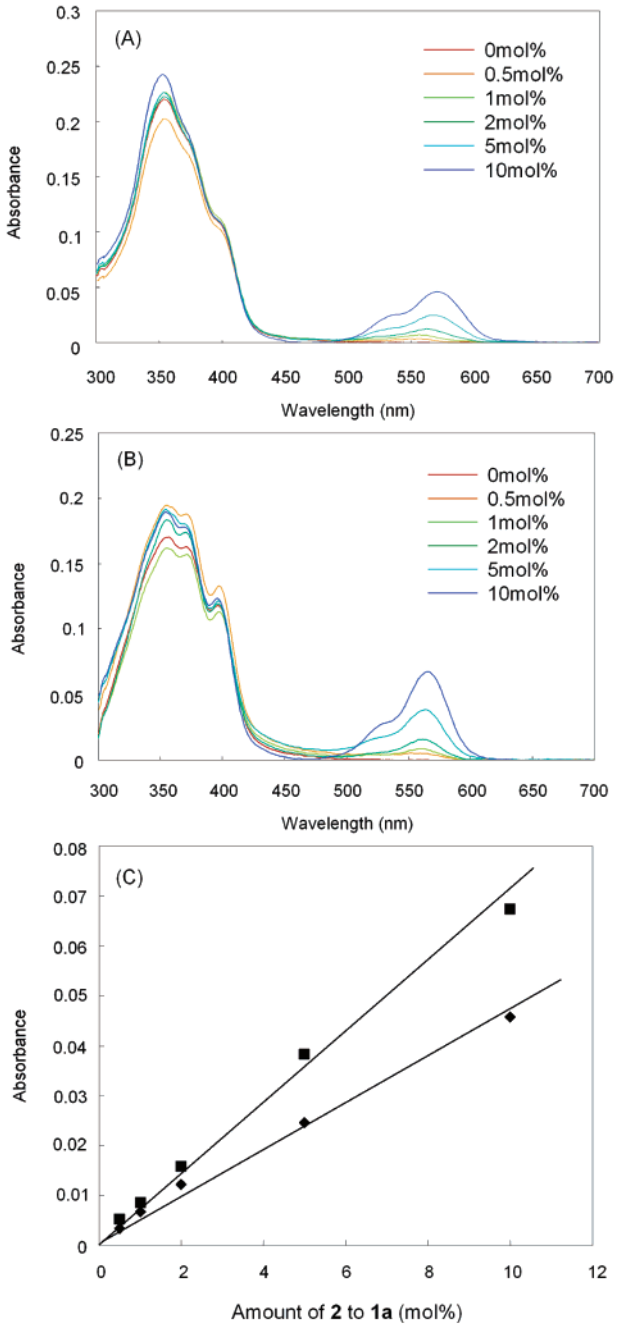

Figure 7. (A) Absorption spectra of oligo(*p*-phenylene vinylene) amphiphile (**1a**)/silicate films and (B) **1a**/poly(2-hydroxyethyl methacrylate) (PHEMA) films doped with rhodamine B derivative (**2**). The amounts of **2** in the precursor solutions were changed from 0 to 10 mol % with respect to the amount of **1a**. (C) Absorption peak maximum of **2** (~560 nm) plotted as a function of concentration of **2** in precursor solutions; ◆: **1a**/silicate film; ■: **1a**/PHEMA film.

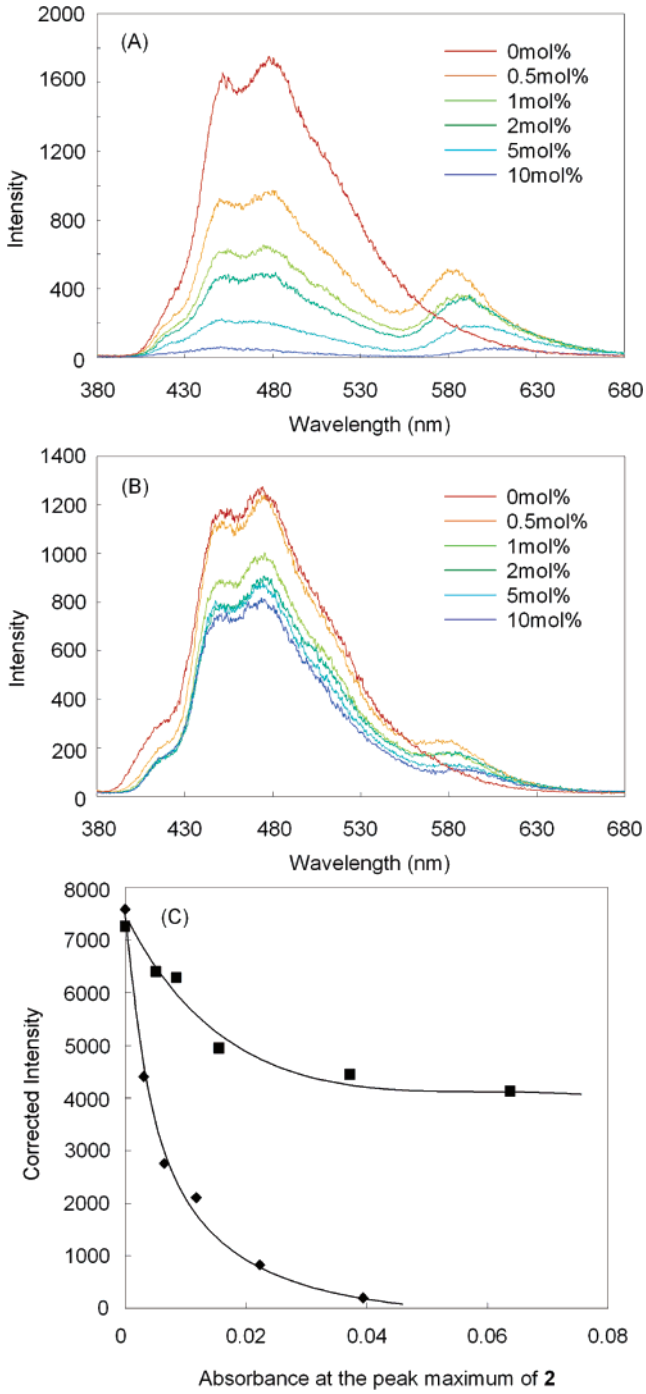

Figure 8. (A) Fluorescence spectra of oligo(*p*-phenylene vinylene) amphiphile (**1a**)/silicate films and (B) **1a**/poly(2-hydroxyethyl methacrylate) (PHEMA) films doped with rhodamine B derivative (**2**). The amounts of **2** in the precursor solutions were changed from 0 to 10 mol % with respect to **1a**. (C) Fluorescence peak intensities of **1a** at 480 nm corrected with the absorbance of **1a** at 350 nm plotted against the absorbance at the peak maximum of **2**; ◆: **1a**/silicate film; ■: **1a**/PHEMA film.

from rhodamine B was monitored at 590 nm, showing the excitation contribution is mostly from OPV absorption around 350 nm and less from direct excitation of the dye around 560 nm.

It has been recently reported that cross-linking in OPV-based materials enhances energy transfer from OPV to rhodamine B compared to mixtures of the two in solution.[20] In this previous work, 50 mol % dye molecules were introduced with respect to OPV in fibrous xerogel films, and quenching of OPV fluorescence and fluorescence from the dye were observed. Although the material investigated is very different from that reported here, it is interesting to point out that in the ordered hybrid films only 0.5 mol % acceptor is necessary to observe quenching of OPV and emission from the rhodamine B derivative. This is 100 times lower than the mol % dye used in the xerogel reported previously.

(20) (a) Ajayaghosh, A.; George, S. J.; Praveen, V. K. *Angew. Chem., Int. Ed.* **2003**, *42*, 332−335. (b) George, S. J.; Ajayaghosh, A. *Chem.−Eur. J.* **2005**, *11*, 3217−3227.

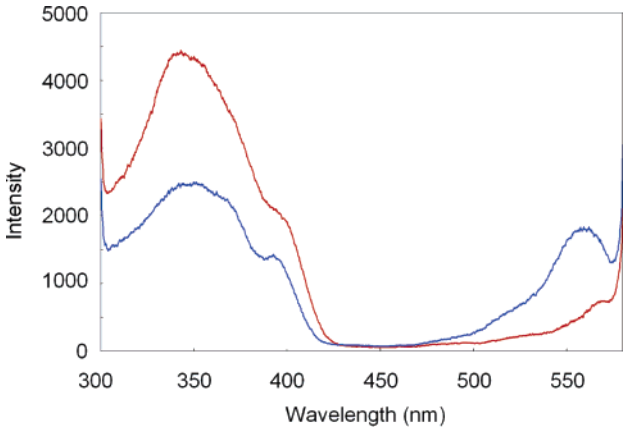

Figure 9. Excitation fluorescence spectra of an oligo(*p*-phenylene vinylene) amphiphile (**1a**)/silicate film (red line) and of a **1a**/poly(2-hydroxyethyl methacrylate) film (blue line) from the precursor solutions containing 2 mol % of **2** (emission wavelength: 590 nm).

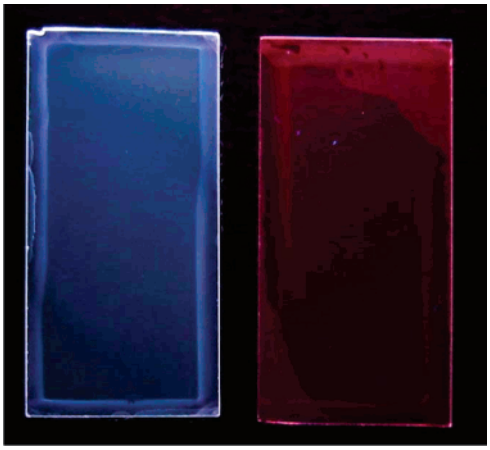

Figure 10. Photographs of oligo(*p*-phenylene vinylene) amphiphile (**1a**)/poly(2-hydroxyethyl methacrylate) film (left) and **1a**/silicate film (right) from precursor solutions containing 2 mol % of rhodamine B derivative (**2**) under UV irradiation ($\lambda = 365$ nm).

Energy Transfer in Disordered Films. To investigate the role of the ordered structure on energy transfer, we prepared amorphous control films with the same OPV amphiphile using a polymer matrix. We used poly(2-hydroxyethyl methacrylate) (PHEMA) instead of silicate because of its good solubility in MeOH. The concentrations of **1a** and **2** in the films were adjusted to make them comparable to the corresponding silicate films. The films obtained were uniform and optically transparent. XRD scans of these **1a**/PHEMA control films did not reveal any peaks, confirming the absence of the periodic structure observed in **1a**/silicate films. When the amount of **2** was increased, the absorption peak corresponding to **2** increased as well, and a red-shift from 556 nm (0.5 mol %) to 566 nm (10 mol %) was observed (Figure 7B). As in the case of silicate films, this can be attributed to the formation of dye dimeric species. The absorbance maximum of **2** scaled linearly with the amount of **2** in precursor solutions (Figure 7C). The greater slope of this curve relative to that of silicate films indicates that **2** was more effectively incorporated into the polymer films. The amount of **2** in the disordered films was estimated using the absorbance at the peak maximum around 560 nm.

Interestingly, the red fluorescence from **2** in the ordered hybrid films was found to be significantly stronger than that in the disordered control films. The difference is visibly striking to the naked eye even when the amount of **2** doped into the films was low. As shown in Figure 10, the **1a**/silicate films deposited on a substrate from a precursor solution with 2 mol % of **2** appears red under irradiation with 365 nm light, whereas the polymer films appear blue under the same irradiation. This could be attributed to both the stronger quenching of the emission from OPV segments and the enhancement of emission from the rhodamine B derivative in the ordered silicate films. The difference in quenching behavior of 480 nm emission in ordered vs disordered films is compared quantitatively in Figure 8C. Excitation spectra of the films with 2 mol % doping of **2** were measured at the emission wavelength of 590 nm (Figure 9). The **1a**/PHEMA films showed a smaller contribution from OPV absorption (around 350 nm) compared with the ordered **1a**/silicate films. Also, the contribution from **2** absorption (around 560 nm) is smaller in the silicate films than in the disordered polymer films. These results suggest a much enhanced energy transfer in the ordered environment of the hybrid films.

The significant enhancement of energy transfer in **1a**/silicate films with nanoscale periodicity could be attributed to several factors. One possible factor is that **2** is dispersed in silicate domains of hybrid films, and thus, the average distance between **1a** and **2** could be shorter than in the PHEMA films. Another possibility is a larger spectral overlap between emission of **1a** and excitation of **2** in the **1a**/silicate films. However, this seems unlikely because the difference in shapes of emission peaks from OPV segments is small between the two types of films (Figure 8A,B). Another factor that may play a role in the enhancement of energy transfer in the ordered hybrid films at a low concentration of dye is efficient energy migration within ordered domains of **1a**. When OPV segments in the hybrid films are excited by irradiation, both energy transfer from **1a** (donor) to **2** (acceptor) and energy migration within **1a** domains could occur. At the low concentration of **2** (0.5 mol % relative to **1a**), the probability of direct energy transfer from **1a** to **2** is expected to be low. However, efficient energy migration in OPV domains of the ordered structure would raise the probability of an acceptor being adjacent to an excited donor, thus significantly enhancing the energy transfer process from **1a** to **2**. In the control polymer films, energy migration within **1a** could be suppressed by the disordered environment, resulting in less efficient energy transfer. This intradomain energy migration and interdomain energy transfer could be features of the efficient energy collecting systems of nature. Future dynamic fluorescence studies on the films would give us more detailed information on the relative importance of various factors in the significant energy transfer observed in the self-assembling hybrid systems studied.

Conclusions

Using self-assembling amphiphiles with electronically active segments and charged groups, we were able to create in a single deposition step an organic−inorganic hybrid film that is periodic at the nanoscale. Extremely efficient energy transfer occurs in these materials from the electronically active segments to dyes grafted covalently to the inorganic silicate domains of the periodic structure. The physical basis of the efficient energy

transfer is possibly related to short distances between donors and acceptors and also efficient energy migration within organic domains. These findings are useful to the design of easily fabricated materials for light emission devices or light harvesting devices in photovoltaic devices.

Experimental Section

General. Unless otherwise noted, all starting materials were obtained from commercial suppliers and used without further purification. ^{1}H NMR spectra were recorded on a Varian Unity 400 (400 MHz) spectrometer using the solvent proton signal as standard. UV−vis spectra were recorded using an HP 8452 spectrometer. Fluorescence spectra were recorded on ISS PC1 Photon Counting Fluorometer using reflection geometry. At least three different points of one sample were measured and averaged to determine the fluorescence intensities from the films. Film thickness of the samples was determined by applying Cauthy model to ellipsometric data in the transparent region recorded on a SOPRA MOSS ES4G spectroscopic ellipsometer. XRD patterns were recorded on a Rigaku RINT 2400 X-ray diffractometer, and infrared spectra were recorded using a Thermo Nicolet Nexus 870 FT-IR spectrometer.

Synthesis. Preparation of OPV/Silicate Hybrid Films. Precursor solutions for the OPV amphiphile/silicate hybrid films were prepared by first dissolving 6.0 mg of **1a** (9.0×10^{-6} mol) in 0.75 mL of MeOH and then adding 15 μL of 35 wt % HCl aqueous solution and 14 μL of tetraethyl orthosilicate (TEOS, 6.25×10^{-5} mol) to the OPV solution. The solutions were stirred for 30 min at room temperature. The final reactant molar ratios were 1 TEOS:0.15 OPV (**1a**): 300 MeOH:8.3 H_2O: 2.5 HCl. The solution was membrane filtered (pore size: 0.45 μm) and deposited on a quartz, glass, or silicon substrate by spin casting at 500−3000 rpm. The films were left overnight at ambient atmosphere and subsequently dried in vacuo for 3 h.

Preparation of Hybrid Films Doped with the Rhodamine B Derivative. The rhodamine B derivative was introduced in the hybrid films by adding **2** (2 mM solution in MeOH) into the precursor solution. The final reactant molar ratios in the precursor solution for the hybrid films with 2 mol % of **2** were 1 TEOS:0.15 OPV **1a**: 0.003 rhodamine B derivative **2**:300 MeOH:8.3 H_2O:2.5 HCl. Films were deposited in the same manner as the undoped hybrid films.

Preparation of the OPV/Polymer Films. OPV amphiphile/polymer films were prepared by using PHEMA instead of TEOS. To the solution of 6.0 mg of **1a** (9.0×10^{-6} mol), PHEMA (5 mg), and the appropriate amount of **2** in 0.75 mL of MeOH was added 15 μL of 35 wt % HCl aqueous solution. The solution was stirred for 30 min at room temperature. **1a**/PHEMA films were prepared by spin casting the precursor solutions at 2000 rpm.

Rhodamine B Derivative Attached Silicate Precursor (2). Rhodamine B derivative **2** was synthesized following the procedure described in ref 17. Rhodamine B isothiocyanate (5.36 mg, 1×10^{-5} mol, 1 equiv) was dissolved in anhydrous MeOH in a dried 5 mL volume flask. 3-aminopropyltriethoxysilane (2.34 μL, 1.1×10^{-5} mol, 1.1 equiv) was added to the solution. The solution was stirred at r.t. for 24 h to afford 2 mM MeOH solution of **2** and used for the sol−gel reaction without further purification. ^{1}H NMR of the material was obtained after the solvent and the excess 3-aminopropyltriethoxysilane were removed in vacuo and the residue was redissolved in DMSO-d_6: δ 8.2−6.3 (m, Ar−H, 9H), 3.75 (m, SiOCH_2CH$_3$), 3.34 (m, 8H), 2.74 (br, 2H), 1.59 (br, 2H), 1.14 (m, SiOCH$_2CH_3$), 1.04 (m, 12H), 0.60 (br, 2H). Broadening of the propylene bridge peaks and a smaller intensity of the triethoxysilane groups were observed, possibly because of partial hydrolysis and condensation of the triethoxysilane groups during the process. Completion of the addition reaction was also confirmed by the disappearance of the characteristic peak for −N═C═S stretching in IR spectra (Nujol, 2050 cm^{-1}).

ω-((Dimethylamino)alkyl)-methanesulfonate Hydrochloride (3a,b). *N*,*N*-Dimethylpropanolamine (4.13 g, 40 mmol, 1 equiv) was dissolved in 100 mL of CH_2Cl_2, and the solution was cooled to 0 °C. Methanesulfonyl chloride (3.7 mL, 48 mmol, 1.2 equiv) was added slowly, and the mixture was stirred for 24 h at r.t. White precipitate was filtered out and dried in vacuo to afford the product **3b** (8.42 g, 97% yield). ^{1}H NMR (DMSO-d_6): δ 10.78 (s, 1H), 4.30 (t, 2H, J = 5.0 Hz), 3.22 (s, 3H), 3.11 (t, 2H, J = 6.0 Hz), 2.73 (s, 6H), 2.08 (m, 2H).

4-(ω-(Dimethylamino)alkoxy)-benzaldehyde (4a,b). 4-Hydroxybenzaldehyde (4.73 g, 38.7 mmol, 1 equiv), **3b** (8.42 g, 38.7 mmol, 1 equiv), potassium carbonate (21.4 g, 155 mmol, 4 equiv), and 18-crown-6-ether (0.95 g, 3.87 mmol, 0.1 equiv) were placed in a flask with a magnetic stirring bar and a cooling column and dissolved in 200 mL of acetone. The mixture was refluxed for 24 h. After cooling, the mixture was filtrated and concentrated in vacuo. The crude product was subjected to a column chromatography using 5% MeOH/CH_2Cl_2 to afford the product **4b** as clear oil (4.47 g, 56%). ^{1}H NMR ($CDCl_3$): δ 9.87 (s, 1H), 7.82 (d, 2H, J = 8.8 Hz), 7.00 (d, 2H, J = 8.2 Hz), 4.10 (t, 2H, J = 6.4 Hz), 2.46 (t, 2H, J = 7.1 Hz), 2.25 (s, 6H), 1.99 (m, 2H).

4-(ω-Bromoalkoxy)-benzaldehyde (5c,d). 4-Hydroxybenzaldehyde (1.22 g, 10 mmol, 1 equiv), 1,6-dibromohexane (3.7 g, 15 mmol, 1.5 equiv), potassium carbonate (2.8 g, 20 mmol, 2 equiv), and 18-crown-6-ether (0.25 g, 1 mmol, 0.1 equiv) were placed in a flask with a magnetic stirring bar and a cooling column and dissolved in 200 mL of acetone. The mixture was refluxed for 24 h. After cooling, the mixture was filtrated and concentrated in vacuo. The crude product was subjected to a column chromatography using CH_2Cl_2 to afford the product **5d** as clear oil (1.7 g, 60%). ^{1}H NMR ($CDCl_3$): δ 9.88 (s, 1H), 7.83 (d, 2H, J = 8.6 Hz), 6.98 (d, 2H, J = 8.5 Hz), 4.05 (t, 2H, J = 6.5 Hz), 3.43 (t, 2H, J = 6.8 Hz), 1.90 (m, 2H), 1.83 (m, 2H), 1.53 (m, 4H).

4-(ω-(Dimethylamino)alkoxy)-benzaldehyde (4c,d). Dimethylamine solution (18 mL, 34.5 mmol, 2.0 M in THF, 5 equiv) was added to **5c** (1.78 g, 6.9 mmol, 1 equiv) at r.t. and stirred for 24 h to give a white suspension. The reaction mixture was washed with H_2O/CH_2Cl_2, and the organic layer was dried and evaporated. The crude product was subjected to a column chromatography using 5% MeOH/CH_2Cl_2 to afford the product **4c** as yellow solid (1.93 g, 61% yield). ^{1}H NMR ($CDCl_3$): δ 9.87 (s, 1H), 7.82 (d, 2H, J = 8.6 Hz), 6.98 (d, 2H, J = 8.6 Hz), 4.06 (t, 2H, J = 6.4 Hz), 2.36 (m, 2H), 2.26 (m, 6H), 1.84 (m, 2H), 1.67 (m, 2H).

Tetraethyl *p*-Xylylenediphosphonate (5). α,α'-Dibromo-*p*-xylene (5.28 g, 20 mmol, 1 equiv) and triethyl phosphite (10.3 mL, 60 mmol, 3 equiv) were placed in a flask with a magnetic stirring bar. A distillation apparatus was attached to collect ethyl bromide formed along with the reaction. The mixture was immersed in an oil bath and heated to 130 °C for 2 h. After cooling, the white crystal was crushed out and recrystalized from hexane to give the product (6.74 g, 89% yield). ^{1}H NMR ($CDCl_3$): δ 7.24 (s, 4H), 4.00 (m, 8H), 3.12 (d, 4H, J = 20.2 Hz), 1.23 (t, 12H, J = 7.0 Hz).

1,4-bis(2-(4-(ω-(Dimethylamino)alkoxyphenyl))−(E)-1-ethenyl) Benzene (6). Compounds **5** (0.72 g, 1.91 mmol, 1 equiv) and **4c** (0.93 g, 4.2 mmol, 2.2 equiv) were dissolved in 100 mL of THF and cooled to 0 °C. *t*-BuOK solution (10 mL, 10 mmol, 1.0 M in *t*-BuOH) was slowly added to the solution with stirring. The reaction mixture was stirred overnight at room temperature and quenched by adding an excess amount of water. White solid precipitated out and was collected by filtration and recrystalized from $CHCl_3$/hexane to afford the product **6c** as a pale-yellow solid (0.72 g, 74% yield). ^{1}H NMR ($CDCl_3$): δ 7.47 (m, 8H), 7.07 (d, 2H, J = 16.1 Hz), 6.96 (d, 2H, J = 16.3 Hz), 6.89 (d, 4H, J = 8.2 Hz), 4.00 (t, 4H, J = 6.0 Hz), 2.33 (t, 4H, J = 7.3 Hz), 2.24 (s, 12H), 1.82 (m, 4H), 1.65 (m, 4H).

1,4-bis(2-(4-(ω-(Trimethylammonium)alkoxyphenyl))−(E)-1-ethenyl) Benzene Dibromide (1). To a suspension of **6c** (0.5 g, 0.98 mmol,

1 equiv) in 100 mL of THF, MeBr solution (5 mL, 10 mmol, 2.0 M in *t*-BuOMe) was added at room temperature. The mixture was stirred overnight, and the white solid was collected by filtration to afford the product **1c** as a pale-yellow solid (0.69 g, 100% yield). ^{1}H NMR (DMSO-d_6): δ 7.54 (m, 8H), 7.21 (d, 2H, J = 16.4 Hz), 7.08 (d, 2H, J = 16.4 Hz), 6.95 (d, 2H, J = 8.47 Hz), 4.04 (t, 4H, J = 5.5 Hz), 3.35 (m, 4H), 3.06 (s, 9H), 1.81 (m, 4H), 1.73 (m, 4H).

Acknowledgment. This work was supported by the U.S. Department of Energy under Award DE-FG02-00ER54810. We are grateful for the use of equipment at the Keck Biophysics Facility, the Jerome B. Cohen X-ray Diffraction Facility, and the Analytical Services Laboratory at Northwestern University.

JA058610S